Railway Gazette
INTERNATIONAL

Ensuring resilience

INFRASTRUCTURE
Whole-system thinking will be key to climate resilience
Page 19

SOUTH KOREA
Seoul embraces 'GTX era' as high speed commuter line opens
Page 40

INTERVIEW
Open access operator optimistic about role in changing UK market
Page 46

Understanding the performance of under sleeper pads

Under sleeper pads have been used for ballast protection and improved track geometry over more than 20 years, but a new contact pressure measurement technique has revealed significant differences in their ballast protection properties.

Dipl-Ing Martin Quirchmair
Research & Development, Getzner Werkstoffe
Dr Harald Loy
R&D Getzner, ITS University Innsbruck
Michael Sehner MSc
Research & Development, Getzner Werkstoffe
Mag Michael Pümpel
Railway Division, Getzner Werkstoffe

Research carried out by universities, manufacturers and railway operators is providing deeper insights into the complex interaction between sleeper and ballast.

Under sleeper pads have been used for ballast protection and to improve track geometry for more than 20 years[1], and the main criterion for categorising USPs is the static bedding modulus. However, it is now becoming apparent that products made from different materials which have the same static bedding modulus can show a significant difference in their ballast protection properties, thanks to a new technique for measuring the contact pressure between the sleeper and the top ballast layer.

Not all USPs are equal

USPs can be used for both ballast protection and vibration mitigation, although the former is by far the more common. USPs can significantly reduce the costs of ballasted track, keeping the track quality at high levels for longer and reducing the need for maintenance, as previously demonstrated by studies into life cycle costs[3]. Tamping cycles can be more than doubled on average, which has a direct impact on the availability of the track.

A UIC leaflet, national regulations and railway standards provide a framework for the use of USPs, which are usually classified as soft, medium or stiff, based on the static bedding modulus.

In Fig 1, the bedding modulus C is required to calculate full surface bearings. In contrast to an ideal spring, which is loaded discretely, a full surface bearing is loaded by a pressure distribution σ0 (x, y). When using the bedding modulus, the normal force F is replaced by the pressure distribution σ0 and the unit is specified in N/m^3, whereas N/mm^3 is often used for elastomers. Put simply, the spring rate is normalised to the surface.

Stiff USPs with a bedding modulus C of greater than 0·25 N/mm^3 are often preferred for open track. Typical examples include ÖBB's SLB 3007 pad (0·36 N/mm^3 according to EN 16730:2016 TC3) and DB's G02/SLB 2210 (0·26 N/mm^3). Both USPs are made of polyurethane with special elasto-plastic properties.

Other materials are also used for ballast protection USPs, including ethylene vinyl acetate copolymer. EVAC is considered equal to the elasto-plastic PUR variants within the scope of a multi-supplier procurement strategy, as it has the same static bedding modulus. However, there are differences between the materials that can be demonstrated in laboratory tests.

Table I. Testing the two USP types

Test	Designation	USP material	Bedding modulus DIN 45673-1
1	PUR V1	Elasto-plastic polyurethane 7 mm	ca. 0·30 N/mm^3
2	EVAC	Ethylen-vinylacetat-copolymer 7 mm	ca. 0·30 N/mm^3
3	PUR V2	Elasto-plastic polyurethane 7 mm	ca. 0·30 N/mm^3
4	no USP	-	-

The four tests included two types of USP with a similar bedding modulus according to DIN 45673-1.

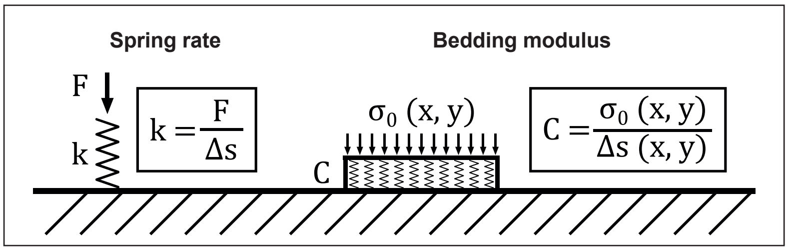

Fig 1. Difference between spring rate k and bedding modulus C, where F is the normal force, σ0 the pressure distribution and Δs the deformation under load.

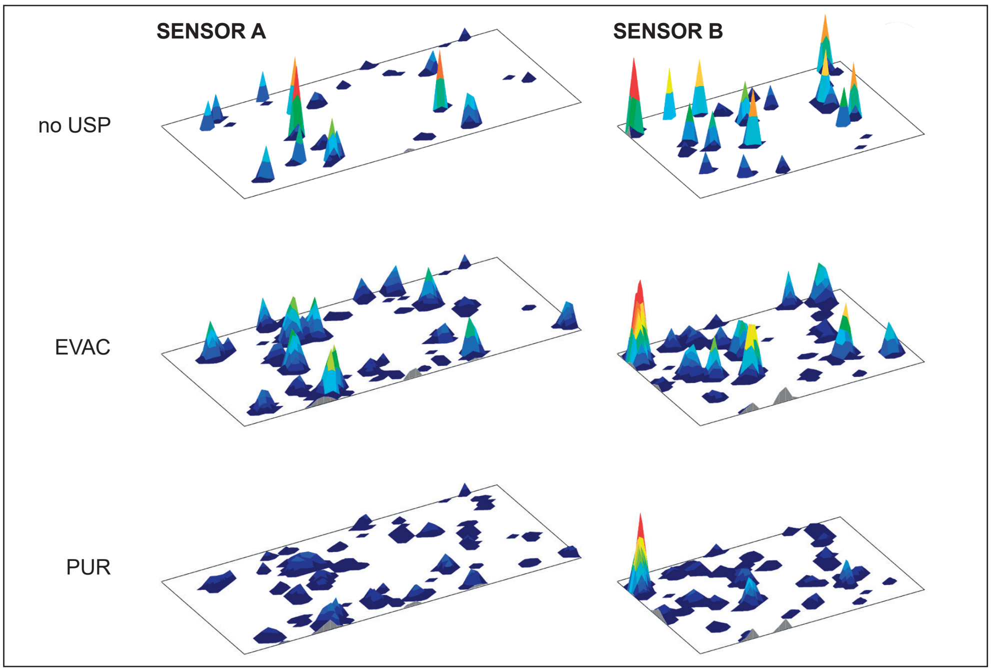

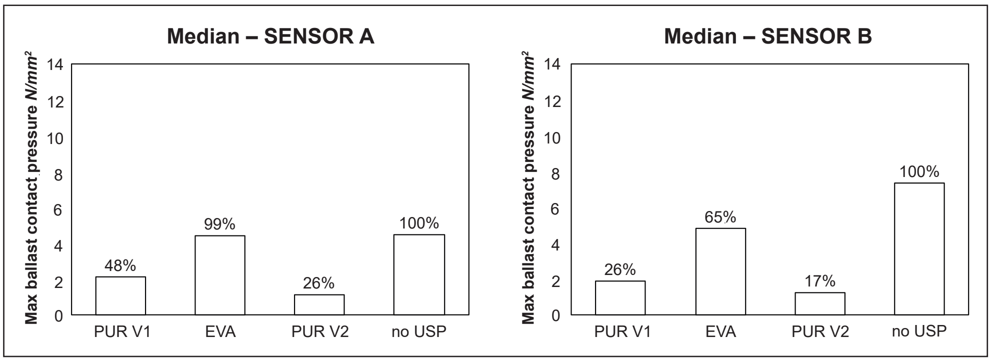

Top: Fig 2. Measured ballast contact pressure peaks on padded and unpadded sleepers under the same load conditions.

Above: Fig 3. Reduction in maximum ballast contact pressures for the tested USPs, based on the median values for evaluation areas 1 to 8 of sensors A and B. The unpadded sleeper serves as a reference in each case.

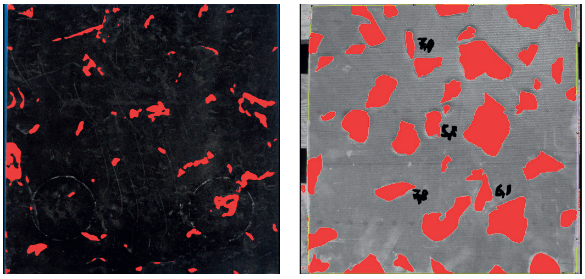

Above: Fig 4. Ballast box testing of the contact area for two USP types. EVAC (left) registered 4·8% of the total area against 22·7% for PUR (right).

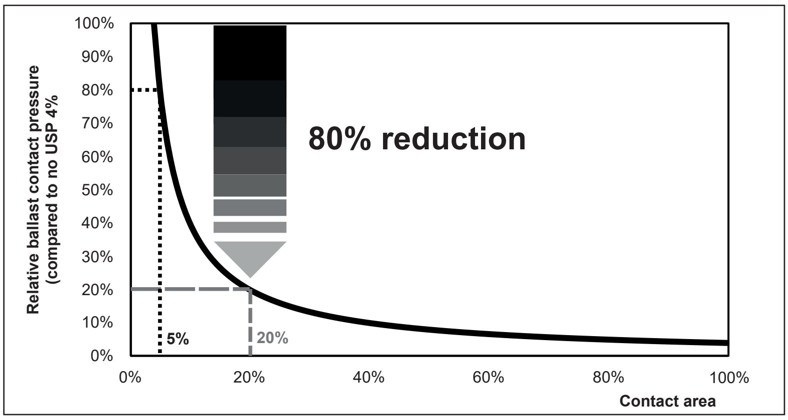

Right: Fig 5. Dependency of the relative average ballast contact pressure on the USP contact area.

Laboratory observations

An initial laboratory test was carried out to determine whether USPs with the same static bedding modulus but made of different materials exhibited different properties. Three scenarios were tested on a concrete sleeper in a ballast box:

- unpadded;
- EVAC pads;
- PUR pads.

The unpadded and EVAC tests were performed once, while that using the PUR pads was done twice, as shown in Table I.

The elasto-plastic properties of PUR enable good embedding of the ballast stones in the USP while providing a high static stiffness. Under cyclic loading, a sensor sleeper[2] was used to measure the contact pressures to which the ballast stones in the topmost layer were directly subjected.

Fig 2 shows that the ballast contact pressures can be influenced by the choice of material, as they are dependent on the ballast contact area of the USP. The additional contact area generated by the plastic properties of the PUR reduces the peaks of the ballast contact pressure by approximately 75% compared with the unpadded scenario. The EVAC pad with an equivalent stiffness achieved a maximum reduction of one third (Fig 3).

Laboratory and track tests have previously been carried out to compare the ballast protection potential of different types of USP. The ballast contact area[4] was typically used to calculate the average contact pressure.

One method was to colour the ballast with a chalk spray and use image analysis to evaluate the imprint made by the ballast under load. This effectively visualised that part of the USP surface that comes into contact with the ballast, so it could be measured.

The contact area of a USP can be determined in the laboratory using ballast or normalised ballast plates, such as a geometric ballast plate according to EN 16730:2016. It can also be seen on sleepers removed from the track, at least to a limited extent. Fig 4 compares the contact area for two materials with the same static stiffness as determined in the ballast box.

Having determined the contact area, it can be combined with the rail seat force (calculated from the bending line of the track structure) and the sleeper geometry in order to estimate the average ballast contact pressure. Fig 5 shows the relation between the contact area and average ballast contact pressure, assuming 100% ballast contact pressure and 4% contact area for the unpadded sleeper. The example

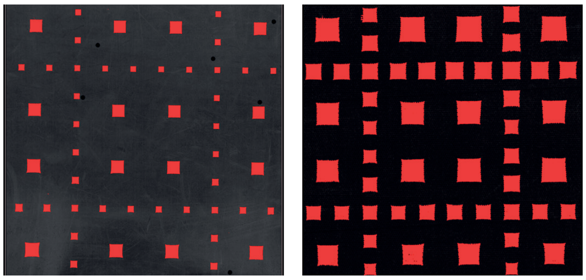

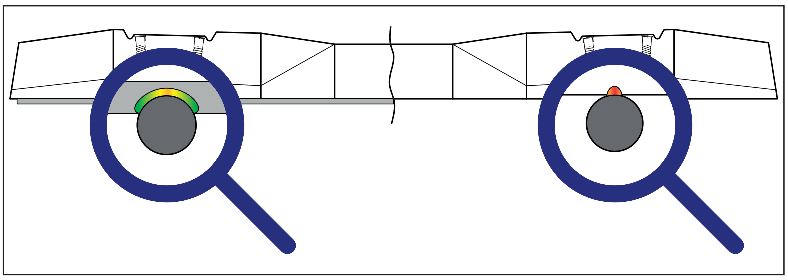

demonstrates that an USP that can achieve a contact area of 20% reduces the average ballast contact pressure by 80%.

This is sufficient for a simple estimation, but it has the disadvantage that it does not take into account the irregular surface of the ballast bed or the geometry of the individual ballast stones.

The problem with averages

In the past, determining the contact area as an interim step for calculating the average ballast contact pressure had several advantages. It was above all simple, as it was merely a case of determining the imprints of the ballast on the pad, and it was easy to compare different materials through characterisation of the contact area.

Developing a standardised measurement method, however, has been a major challenge. There are no standards or internationally recognised guidelines that define a procedure for determining the contact area. The area is also dependent on the type of ballast, its distribution and the forces being applied.

To evaluate products from both a qualitative and quantitative perspective, Getzner Werkstoffe developed its own procedure back in 2014[5]. This is based on EN 16730:2016 and uses a geometric ballast plate for defined loading. This ensures that products made from different materials are always tested with the same forces and load cycles (Fig 6).

However, there is still a fundamental problem. The ballast stones are not flat but angular, and they protrude out of the topmost layer of ballast by different amounts. In the simple model, each contact point between the ballast and the bottom of the sleeper is included to the same extent, regardless of whether it is supporting a high or low load. But the pressure distribution on individual ballast stones is not homogeneous, as shown schematically in Fig 7.

In reality, each stone is individually arranged and supports the load to a different extent. The ballast is most likely to degrade at the positions where the contact pressures are highest. So rather than determining the contact pressures indirectly via the contact area,

Above left: *Fig 6. Contact area as determined in the laboratory for USPs with the same static stiffness. Left: EVAC (5·3%); right: PUR (20·8%).*

Above right: *Fig 7. Schematic representation of the pressure distribution/load on an idealised ballast stone (sphere), padded on the left and unpadded on the right.*

can we measure them directly at the interface between ballast and sleeper? This is where the sensor sleeper technology comes in.

Direct measurement

Getzner's prototype sensor sleeper was first used on an ÖBB test track in 2018[6]. Since then, the system has been used in a demonstrator turnout within the scope of a Shift2Rail project[7] and in laboratory tests for comparing simulation models.

A thin sensor element is glued onto the sleeper, facing the ballast. Within this area, pressures can be continuously recorded in a grid of 2 288 points with a spatial resolution of 9·3 mm by 4·7 mm.

The sensor sleeper technology can

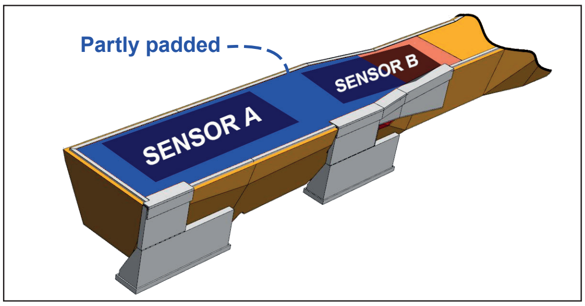

Fig 8. First-generation sensor sleeper with L2 sleeper geometry.

Fig 9. Setup for the entire sleeper test in the ballast box, showing the wired sensor sleeper technology at the nearer end of the concrete sleeper.

be used both with and without USPs, making it an ideal measuring instrument for comparing different USPs.

The following tests were undertaken with a first generation sensor, mounted on a type L2 sleeper (Fig 8). The sleeper was only partially padded during the measurements — because it was also being used within the scope of another research project. This did not create any restrictions on the laboratory tests, as only the padded area was evaluated, and the middle unpadded section was not in contact with the ballast in all configurations.

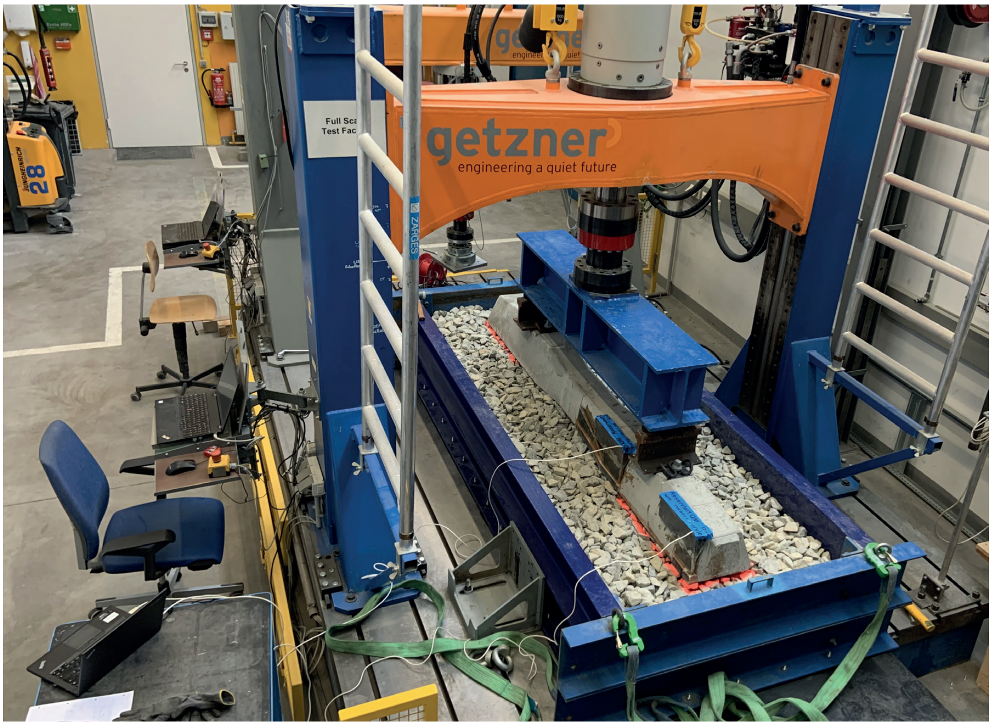

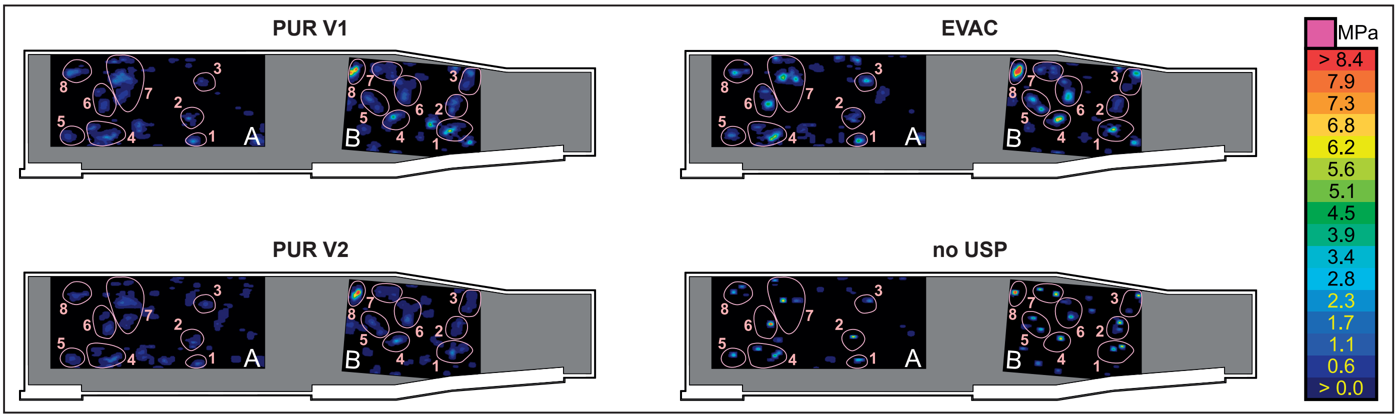

Top: Fig 10. Measured pressure distributions and selected evaluation areas 1 to 8 per sensor.

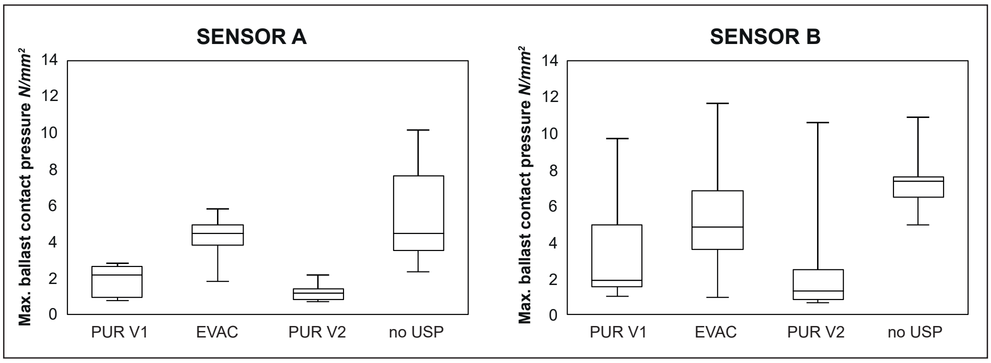

Above: Fig 11. Maximum ballast contact pressure on evaluation areas 1 to 8 for sensors A and B as recorded in laboratory testing.

Concept and test setup

The L2 sleeper sensor system was tested in the ballast box according to EN 16730:2016, Annex M. The box was 3 m long and 1 m wide, and was filled with ballast up to a height of 350 mm. Ballast was added in two layers, each being compacted using a vibrating plate. The sleeper was then laid in the centre of the compacted ballast, so that the middle section of the sleeper was not in contact with the ballast (Fig 9).

The position of the sleeper on the ballast was marked, and the ballast bed was not changed between tests. The objective was to disturb the ballast bed as little as possible, in order to ensure a similar contact between sleeper and ballast for all test scenarios.

During each test, a sinusoidal load between 5 kN and 100 kN was applied at a frequency of 5 Hz for 2 h (36 000 cycles). For ease of comparison, the same upper load of 100 kN was chosen for both padded and unpadded sleepers. The additional activation of the bending line due to the elasticity of the USP would otherwise have resulted in a reduction in the upper load in comparison with the unpadded scenario. The frequency was then immediately reduced to 0·5 Hz and the pressure distribution on the bottom of the sleeper was recorded.

Three setups were selected for the analysis — one unpadded scenario and two 7 mm thick 'stiff' USPs made of different materials; EVAC and elasto-plastic PUR.

The test with the elasto-plastic PUR was performed twice as shown in Table I, but statistical reliability could not be achieved. The test represents a first comparison using the new procedure.

Measurement results

The measured pressure distributions for the test scenarios are indicated in Fig 10. Eight areas per sensor were defined for the evaluation. As the ballast was manipulated as little as possible between the individual tests, the support points of the ballast stones carrying the load were in identical positions in all load cases. A clear difference between the individual scenarios can already be seen, based on the colouring of the ballast contact pressures.

Areas with maximum ballast contact pressure have the highest probability of ballast stone fracturing, and can thus be used as the basis for evaluating the ballast protection properties of a USP.

The maximum pressure values for each evaluation area were then compared. The irregularity of the ballast can result in individual outliers, whereby a single stone carries a significant above-average load. This was the case at point 8 on sensor B, for example. To ensure these outliers do not give too much weight in the evaluation, a median of the eight areas was used to benchmark the different USPs against each other. The median maximum ballast contact pressures for the two sensors is shown in Fig 11.

Despite the irregularity of the ballast, a result of a similar quality was achieved for sensors A and B. The outlier at point 8 of sensor B stands out in all scenarios, and is also reflected in the maximum values in Fig 11.

The first prototype test demonstrated that the EVAC USP exhibited a reduction of the maximum ballast contact pressure relative to the unpadded

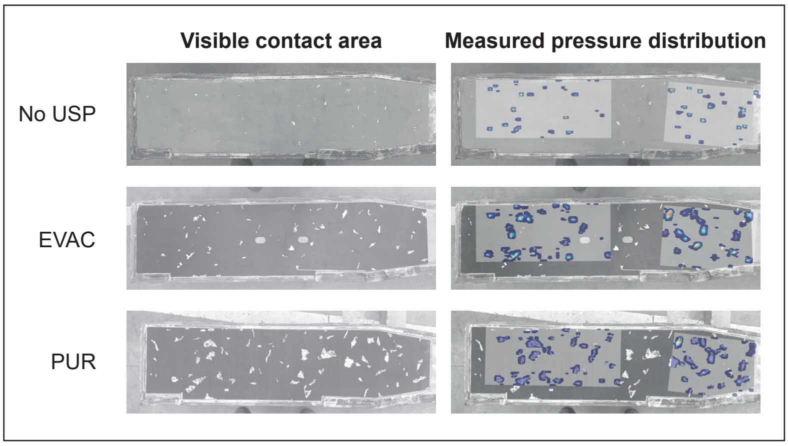

Fig 12. Comparison of the visible ballast imprints with the measured pressure distributions under same load conditions.

sleeper of one third or less, using the median evaluation. By contrast, the PUR pad, which was tested twice, reduced the ballast contact pressure by at least half and mostly 75% or more.

Alternative evaluation methods

The new sensor technology makes it possible to assess the load transfer of the individual ballast stones depending on various superstructure configurations. Not only can it evaultate the number of ballast stones in contact with the bottom of the sleeper but also the homogeneity of the load distribution. Comparison of the visible ballast imprints after the test with the measured pressure images confirmed that each ballast stone was supporting a different load (Fig 12).

In general, ballast protection is achieved by distributing the force over as large a contact area as possible. This can be realised by embedding the ballast stones in the USP and by activating multiple ballast stones by means of elastic and plastic properties. The plastic behaviour of the USP ensures good embedding, even at high stiffness.

This could also be used as the basis for a possible evaluation method. The measured pressure distribution is displayed as a cumulative sum chart, and the force components plotted as a percentage on the y-axis. The chart thus shows the percentage of the total force that is transferred up to the ballast contact pressure p shown on the x-axis.

The task of the USP is to transfer as much of this total force as possible at low ballast contact pressures, and prevent the ballast from being overloaded. A sharp increase in the relative share of force at low pressures is therefore an indicator of good ballast protection properties (Fig 13). Once again, it is clear to see the advantages of the elasto-plastic behaviour of the PUR USPs, where the load is predominantly transferred at low pressures.

Stability in the track

In the past, both lateral measurements in the laboratory[8] and lateral resistance measurements in the track[9] demonstrated that good embedding of the ballast stones in the USP also has an impact on the lateral stability of the track.

Laboratory tests with unconsolidated and consolidated concrete blocks were carried out as part of a bachelor's thesis. The equivalent pad types were used as for the sensor sleeper tests. It is clear in Fig 14 that the embedding of the ballast stones in PUR resulted in a considerable increase in the resistance to lateral pushing in both the unconsolidated and consolidated state. The weaker embedding of ballast stones in EVAC, by contrast, resulted in less of an increase and produced values comparable with the unpadded scenario.

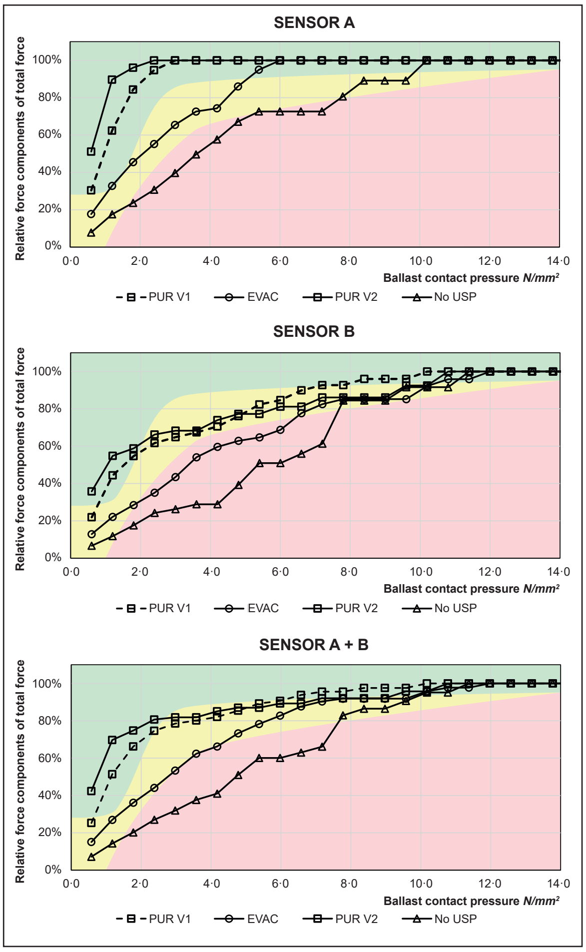

Fig 13. Relative shares of total force transferred by the tested USPs depending on the ballast contact pressure (displayed as a cumulative chart, whereby a high load transfer at low pressures corresponds to good ballast protection).

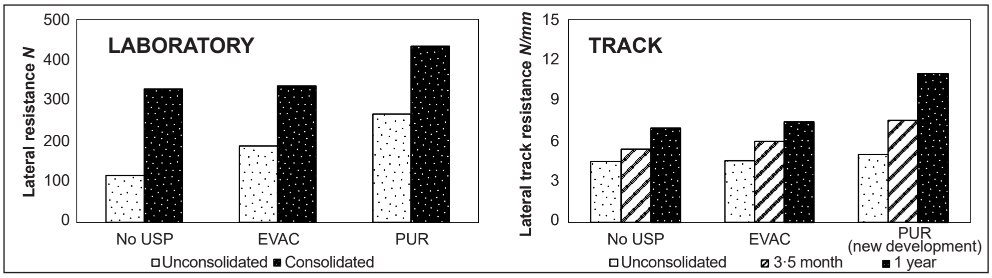

Fig 14. Lateral resistance measurements in the laboratory (left) and in track (right) both showed the superiority of the PUR pads.

A similar result could be seen in the track. USPs made from EVAC and PUR (optimised for stability) were installed in a narrow-gauge track in Niederösterreich, and measurements were performed by the University of Innsbruck. Fig 14 shows that a significant increase in lateral resistance was only achieved with the PUR USPs.

Outlook

Our work suggests that conventional methods for evaluating USPs cannot take into account all of properties relevant to the ballast superstructure, and further work is needed to expand the evaluation criteria through both laboratory investigations and field trials.

These studies could form the basis for a more targeted development and optimisation of products for specific applications, which should gradually contribute to making the ballast and track superstructure more economical and sustainable.

References

1. IRS 70713-1: Bahnanwendungen — Oberbau & Konstruktive Ingenieurbauwerke "Schwellensohlen (USP) — Empfehlungen für die Verwendung", 2nd edition, 2019-12
2. Sehner M, Augustin A, Quirchmair M and Loy H. Sensorschwellentechnologie: Ein Blick zwischen Schwelle und Schotter, (*ZEVrail* 8/2023)
3. Veit P and Marschnig S. Towards a more sustainable track. (RG 1.11 p42)
4. Iliev D. Die horizontale Gleislagestabilität des Schotteroberbaus mit konventionellen und elastisch besohlten Schwellen, Doctoral thesis, TU München, January 2012
5. Getzner Werkstoffe: WI 22202 Determination of Contact Area of USP, Internal work instruction, dated 19/09/2019
6. Getzner Werkstoffe: Sensorschwellen — Messung der Pressungen unter Spannbetonschwellen L2 und L17, Report 2021-088, 27/07/2021
7. Projects conducted by the first European rail initiative, Shift2Rail. **https://projects.shift2rail.org**
8. Gabl S: Einfluss der Kontaktfläche auf den Querverschiebewiderstand, Bachelor's thesis, University of Applied Sciences, St. Pölten, August 2019
9. Steiner E and Krueger M. Verwerfungssichere durchgehend verschweißte Schmalspurgleise bei der Mariazellerbahn der Niederösterreich Bahnen (NÖVOG), *Eisenbahntechnische Rundschau Austria*, September 2022